npj | quantum materials

Article

Published in partnership with Nanjing University

https://doi.org/10.1038/s41535-024-00672-0

Majorana modes in striped two-dimensional inhomogeneous topological superconductors

Pasquale Marra [1,2] ✉, Daisuke Inotani[2], Takeshi Mizushima [3] & Muneto Nitta[2,4]

Majorana zero modes have gained significant interest due to their potential applications in topological quantum computing and in the realization of exotic quantum phases. These zero-energy quasiparticle excitations localize at the vortex cores of two-dimensional topological superconductors or at the ends of one-dimensional topological superconductors. Here we describe an alternative platform: a two-dimensional topological superconductor with inhomogeneous superconductivity, where Majorana modes localize at the ends of topologically nontrivial one-dimensional stripes induced by the spatial variations of the order parameter phase. In certain regimes, these Majorana modes hybridize into a single highly nonlocal state delocalized over spatially separated points, with exactly zero energy at finite system sizes and with emergent quantum-mechanical supersymmetry. We then present detailed descriptions of braiding and fusion protocols and showcase the versatility of our proposal by suggesting possible setups that can potentially lead to the realization of Yang-Lee anyons and the Sachdev-Ye-Kitaev model.

Majorana modes (MMs) localized at the vortex cores of two-dimensional (2D) or at the ends of one-dimensional (1D) topological superconductors (TSs)[1–7] are potential building blocks for topological quantum computing[8–11] and other exotic quantum systems that effectively simulate high-energy theories such as supersymmetry (SUSY)[12–19] and synthetic horizons in the Sachdev-Ye-Kitaev (SYK) model[20–22] (see also refs. 23–36). Specifically, 2D TSs[1] realized with topological insulator (TI) or quantum spin Hall insulator/superconductor heterostructures[3], transition metal dichalcogenides[37,38], iron pnictides[39–41] or other oxypnictide superconductors[42], or magnet-superconductor hybrid systems[43–46] may provide a flexible platform to exploit the nonabelian exchange statistics of MMs[8], due to the ability to manipulate vortex cores in a 2D space, and detect them through scanning tunneling microscopy. Conversely, 1D TSs[2], e.g., proximitized quantum wires[6,7,47–49] arranged in 2D networks, offer a simplified but less flexible setup to perform braiding[50–52].

To combine the flexibility of braiding in 2D with the conceptual simplicity of 1D platforms and overcome their limitations, here we introduce topologically nontrivial stripes (TNSs) induced by inhomogeneous superconducting states[53–55] where the gauge-invariant phase rotates in a regular pattern. The rotating phase effectively generates quasi-1D structures within the 2D system, where the topological invariant assumes alternatively trivial and nontrivial values as a function of the phase. This results into a *striped* 2D TS with emergent TNSs equivalent to 1D TSs, localized at 1D lines where the order parameter phase is homogeneous and the topological invariant is nontrivial, so that a quasi-1D topological superconducting state emerges. Here, pointlike (0D) MMs localize at the ends of the TNSs, whose distance and direction can be manipulated by varying the in-plane field magnitude and direction. These highly nonlocal MMs offer multiple and flexible ways to implement braiding due to the possibility of moving and rotating the stripes in a 2D space.

Specifically, we consider a TI film in a magnetic field[56–58] where the surface states are gapped out by proximity with a conventional superconductor, allowing the realization of second-order TSs[59] with Majorana hinge modes. We show that these (1D) Majorana hinge modes transmute into pointlike (0D) Majorana corner modes localized at the end of TNSs induced by an inhomogeneous superconducting order. Hence, we describe braiding and fusion protocols implemented by joining, splitting, and moving stripes via external gates or magnetic force microscopy, and rotating them by rotating the magnetic field. Furthermore, we show how configurations with several stripes induce a regularly-spaced array of MMs, realizing emergent quantum mechanical SUSY, zero-energy multi-locational MMs[60] delocalized on multiple spatially separated points, Yang-Lee

[1]Graduate School of Mathematical Sciences, The University of Tokyo, Meguro, Tokyo, Japan. [2]Department of Physics & Research and Education Center for Natural Sciences, Keio University, Yokohama, Kanagawa, Japan. [3]Department of Materials Engineering Science, Osaka University, Toyonaka, Osaka, Japan. [4]International Institute for Sustainability with Knotted Chiral Meta Matter (SKCM2), Hiroshima University, Higashi-Hiroshima, Hiroshima, Japan.
✉e-mail: pmarra@ms.u-tokyo.ac.jp

anyons[61] with non-unitary and nonabelian statistics, and the SYK model[22] reproducing the maximally-chaotic dynamics of black holes.

Results

Creation of topologically nontrivial stripes

The boundary mean-field Hamiltonian describing the proximitized surface states at the top and bottom of a TI in a magnetic field as sketched in Fig. 1a is[56–58,62]

$$\mathcal{H} = \int \mathrm{d}\mathbf{r}\, \psi^\dagger(\mathbf{r}) H \psi(\mathbf{r}) - \sum_\tau \left(\Delta_\tau(\mathbf{r}) \psi_{\tau\downarrow}(\mathbf{r}) \psi_{\tau\uparrow}(\mathbf{r}) + \mathrm{h.c.} \right) + \tfrac{1}{U} \int \mathrm{d}\mathbf{r} \sum_\tau |\Delta_\tau(\mathbf{r})|^2, \quad (1)$$

where $\psi(\mathbf{r}) = \left[\psi_{1,\uparrow}(\mathbf{r}), \psi_{1,\downarrow}(\mathbf{r}), \psi_{2,\uparrow}(\mathbf{r}), \psi_{2,\downarrow}(\mathbf{r}) \right]^\intercal$ are the electron field operators with $\uparrow\downarrow$ indexes for spin, $\tau = 1, 2$ for pseudospin (i.e., top and bottom surfaces) and

$$H = (m' \mathbf{p}^2 + m)\tau_x - v\mathbf{p} \times \boldsymbol{\sigma} \tau_z - \mu + \mathbf{b} \cdot \boldsymbol{\sigma}, \quad (2)$$

where m and m' are the tunneling parameters depending on the layer thickness[56,63], v the Dirac cone velocity, $\mathbf{p}$ the momentum on xy plane, $\mathbf{b}$ the Zeeman field, μ the chemical potential, and σ_i, τ_i the Pauli matrices in spin and pseudospin space. Here, $\Delta_\tau(\mathbf{r})$ is the mean-field order parameter of the surface states, i.e., at the interface between the superconductor and the TI, and which can be calculated self-consistently[58,64,65] as $\Delta_\tau(\mathbf{r}) = -U\langle 0|\psi_{\tau\downarrow}(\mathbf{r})\psi_{\tau\uparrow}(\mathbf{r})|0\rangle$,where U the superconducting pairing strength describing the on-site electron-electron attractive interaction within the surface states. In the normal regime with unbroken time-reversal symmetry (i.e., $\Delta = b = 0$), the Hamiltonian is unitarily equivalent[56,63] to the Bernevig, Hughes, and Zhang model for a 2D quantum spin Hall TI[66] with energy dispersion having two spin-degenerate branches with gap $2|m|$ at zero momentum and a topologically nontrivial phase for $mm' < 0$. The TI surface states exhibit a gap $2(b - |m|)$ at zero momentum for $b \neq |m|$ and remain gapped at finite momenta for finite out-of-plane fields $b_z > 0$.

Superconductivity emerges when the Cooper instability opens a gap at the Fermi level lying within the conduction band, assuming $|\mu| > b - |m|$. The symmetry between the top and bottom surfaces mandates $|\Delta_1(\mathbf{r})| = |\Delta_2(\mathbf{r})|$. Hence, by choosing a gauge where the phases of the order parameter on the top and bottom surfaces are opposite, one can write $\Delta_1(\mathbf{r}) = \Delta_2(\mathbf{r})^*$ up to a gauge transformation. We can thus write $\Delta_1(\mathbf{r}) = \Delta(\mathbf{r}) = |\Delta(\mathbf{r})|e^{i\phi(\mathbf{r})}$ and $\Delta_2(\mathbf{r}) = \Delta(\mathbf{r})^* = |\Delta(\mathbf{r})|e^{-i\phi(\mathbf{r})}$, where $2\phi(\mathbf{r})$ is the gauge-invariant phase difference between top and bottom surfaces. The mean-field Bogoliubov-de Gennes Hamiltonian is $\mathcal{H}_{\mathrm{BdG}} = \frac{1}{2}\int \mathrm{d}\mathbf{r}\, \Psi^\dagger(\mathbf{r}) \cdot H_{\mathrm{BdG}} \cdot \Psi(\mathbf{r})$ with

$$H_{\mathrm{BdG}} = \left[(m'\mathbf{p}^2 + m)\tau_x - v\mathbf{p} \times \boldsymbol{\sigma}\tau_z - \mu \right] v_z + \mathbf{b} \cdot \boldsymbol{\sigma} + |\Delta(\mathbf{r})| \left[\cos(\phi(\mathbf{r}))\, v_x + \sin(\phi(\mathbf{r}))\, \tau_z v_y \right], \quad (3)$$

where $\Psi(\mathbf{r}) = \left[\psi(\mathbf{r}), \sigma_y \psi^\dagger(\mathbf{r}) \sigma_y \right]^\intercal$, and v_i the Pauli matrices in particle-hole space.

Let us first assume uniform superconducting pairing $\Delta(\mathbf{r}) = \Delta e^{i\phi}$ with $\Delta > 0$. Topologically nontrivial phases with particle-hole symmetry and broken time-reversal symmetry (class D) in 2D are labeled by the Chern number of the quasiparticle excitation gap $c \in \mathbb{Z}$. The gap closes when $|m^2 + \mu^2 + \Delta^2 - b^2| = 2|m|\sqrt{\mu^2 + \Delta^2 \sin^2\phi}$, and remains open at finite momenta for $b_z \neq 0$ and $\phi \neq 0$. For $\phi = \pi/2$, the quasiparticle excitation gap $2\min(||m| - |b \pm \sqrt{\mu^2 + \Delta^2}||)$ closes at zero momentum with a quantum phase transition each time that any of the quantities $b \pm m \pm \sqrt{\mu^2 + \Delta^2}$ change sign. This condition divides the parameter space into topologically distinct phases separated by the closing of the quasiparticle excitation gap, where we calculate the Chern number numerically[67]: We thus found a trivial phase at weak fields, where $|m| > b + \sqrt{\mu^2 + \Delta^2}$ or $\sqrt{\mu^2 + \Delta^2} > b + |m|$, a nontrivial phase with $|c| = 2$ at strong field $b > |m| + \sqrt{\mu^2 + \Delta^2}$, and a nontrivial intermediate phase with $|c| = 1$ where no energy scale dominates, i.e., when $|m| + \sqrt{\mu^2 + \Delta^2} > b > ||m| - \sqrt{\mu^2 + \Delta^2}|$, or equivalently $b + |m| > \sqrt{\mu^2 + \Delta^2} > |b - |m||$, or $b + \sqrt{\mu^2 + \Delta^2} > |m| > |b - \sqrt{\mu^2 + \Delta^2}|$. The nontrivial phases persist for $\phi \neq \pi/2$ as long as the quasiparticle excitation gap remains open (see also Supplementary Note 2). The parity of the topological invariant[68,69] $\nu = c \bmod 2$ is given by $(-1)^\nu = \prod_{\mathbf{k}} \mathrm{sgn}\left(\mathrm{pf}\left(H_{\mathrm{BdG}}(\mathbf{k}) \sigma_y v_y \right) \right)$ where $H_{\mathrm{BdG}}(\mathbf{k})$ is the Hamiltonian density as a function of the momentum eigenvalues k with the product spanning over the time-reversal symmetry points of the Brillouin zone, giving

$$(-1)^\nu = \mathrm{sgn}\left(|m^2 + \mu^2 + \Delta^2 - b^2| - 2|m|\sqrt{\mu^2 + \Delta^2 \sin^2\phi} \right). \quad (4)$$

Since the effective boundary Hamiltonian in Eq. (2) describes the surface states of a 3D TI, these nontrivial gapped phases are 3D second-order TS with Majorana hinge modes, i.e., gapless modes on the hinges[59], as in Fig. 1b.

For zero magnetic fields or fields parallel to the z-axis, the SO(2) rotational symmetry in the xy plane is unbroken: this allows the creation of

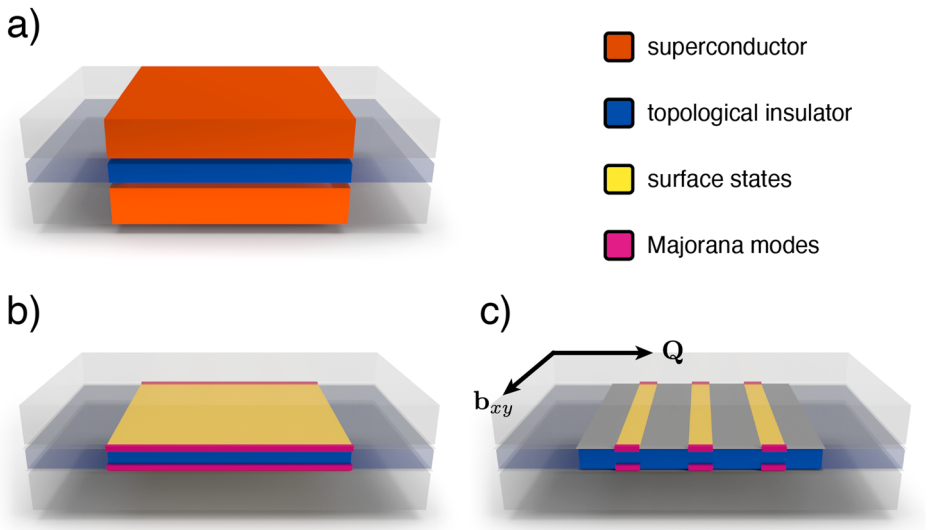

Fig. 1 | Topological insulator film with top and bottom surfaces proximitized by conventional superconductors. a Topological insulator film sandwiched between two conventional superconductors. **b** Majorana hinge modes in the nontrivial phase at finite field and uniform pairing (we removed the superconductors for clarity). **c** Topologically nontrivial stripes and Majorana corner modes in the nonuniform superconducting phase. The LO order parameter is modulated as $\Delta(\mathbf{r}) \propto e^{i\mathbf{Q}\cdot\mathbf{r}}$. The Cooper pairs momentum $\mathbf{Q}$ is perpendicular to the in-plane magnetic field $\mathbf{b}_{xy}$.

Cooper pairs with zero momentum $Q = 0$ formed by electrons with opposite spin and opposite momenta. However, in the presence of a finite spin-orbit coupling term $\propto \mathbf{p} \times \boldsymbol{\sigma}$, a finite in-plane magnetic field $\mathbf{b} \cdot \boldsymbol{\sigma}$ (Zeeman term) shift electrons with opposite spin in opposite directions $\mathbf{k} \to \mathbf{k} \pm \mathbf{Q}/2$, with the momentum $\mathbf{Q}$ perpendicular to the in-plane field and $Q \approx 2b_{xy}/v$ at large fields. In the Pauli limit, neglecting the orbital pair-breaking mechanism, this allows the creation of Cooper pairs with finite momentum $\mathbf{Q}$, formed by electrons with opposite spin and momentum eigenvalues $\mathbf{k}$ and $-\mathbf{k} + \mathbf{Q}$, described by a nonuniform order parameter $\Delta(\mathbf{r})$ that depends periodically in space with a wavelength $\lambda = 2\pi/Q$. The simplest spatial dependence compatible with the symmetries of the system considered here[58] is

$$\Delta(\mathbf{r}) = \Delta_0[\cos\theta \cos(\mathbf{Q}\cdot\mathbf{r}) + \mathrm{i}\sin\theta \sin(\mathbf{Q}\cdot\mathbf{r})], \tag{5}$$

with $\Delta_0 > 0$ and $0 \le \theta \le \pi/2$ (up to a gauge transformation) determined by the minimum of the free energy $\mathcal{F} = \langle \mathcal{H} \rangle$ at zero temperature. The order parameter has a total magnitude $|\Delta(\mathbf{r})| = \Delta_0\sqrt{(1+\cos(2\theta)\cos(2\mathbf{Q}\cdot\mathbf{r}))/2}$, having minima and maxima for any $\theta \neq \pi/4$ along the 1D planes parallel to the in-plane field, which we call respectively nodal and antinodal lines, satisfying $\mathbf{Q}\cdot\mathbf{r} = n\pi/2$ for $n \in \mathbb{Z}$. Its phase $\phi(\mathbf{r}) = \arg\Delta(\mathbf{r})$ is spatially modulated if $\theta \neq 0, \pi/2$, being $\tan(\phi(\mathbf{r})) = \tan\theta \tan(\mathbf{Q}\cdot\mathbf{r})$ giving $\sin^2(\phi(\mathbf{r})) = 0, 1$ for $\mathbf{Q}\cdot\mathbf{r} = n\pi/2$. One can verify that $\Delta(\mathbf{r}, -\theta) = \Delta(\mathbf{r}, \theta)^*$, $\Delta(\mathbf{r}, \pi/2 - \theta) = -\Delta(\mathbf{r}, \pi/2+\theta)^*$, and that $\Delta(\mathbf{r}, \pi/4 - \theta) = \mathrm{i}\Delta(\mathbf{r}', \pi/4 + \theta)^*$ with $\mathbf{r}' = \pi\mathbf{Q}/2Q^2 - \mathbf{r}$. Consequently, $H(\alpha + \theta)$ and $H(\alpha - \theta)$ are unitarily equivalent and thus have the same energy spectra, which mandates $\mathcal{F}(\alpha + \theta) = \mathcal{F}(\alpha - \theta)$ for $\alpha = 0, \pi/4, \pi/2$. This mandates the presence of stationary points $\delta\mathcal{F}(\theta) = 0$ for $\theta = 0, \pi/2$, and $\pi/4$ (see also Supplementary Note 3). The cases $\theta = 0, \pi/2$ correspond to Larkin-Ovchinnikov (LO) orders with a constant phase $\phi(\mathbf{r}) = 0, \pi/2$ and magnitude $\Delta_0|\cos(\mathbf{Q}\cdot\mathbf{r})|$ and $\Delta_0|\sin(\mathbf{Q}\cdot\mathbf{r})|$, respectively, which becomes zero at the nodal lines and reaches its maximum Δ_0 at the antinodal lines. The case $\theta = \pi/4$ instead corresponds to a Fulde-Ferrel (FF) order with a constant magnitude $\Delta_0/\sqrt{2}$ and a phase $\phi(\mathbf{r}) = \mathbf{Q}\cdot\mathbf{r}$ giving $\sin^2(\phi(\mathbf{r})) = 0, 1$ respectively for $\mathbf{Q}\cdot\mathbf{r} = n\pi$ and $\mathbf{Q}\cdot\mathbf{r} = \pi/2 + n\pi$. The 1D lines defined by constant $\mathbf{Q}\cdot\mathbf{r}$ have constant order parameter $\Delta = \Delta(\mathbf{r})$ and are described by an effective 1D Hamiltonian $H_{1D}(r) = \left[-vp_x\sigma_y\tau_z + (m/p_x^2 + m)\tau_x\right]v_z + \mathbf{b}\cdot\boldsymbol{\sigma} - \Delta_0\tau_z v_y|\Delta|(\cos\phi\, v_x + \sin\phi\,\tau_z v_y)$, for in-plane fields in the x direction, which is equivalent to Eq. (3) when one takes $p_y = 0$. In symmetry class D in 1D, topologically inequivalent phases are labeled by a $\nu \in \mathbb{Z}_2$ topological invariant. By dimensional reduction, ν must coincide with the parity of the topological invariant in 2D defined in Eq. (4): Hence, there is only one nontrivial phase in 1D, realized when $\nu = 1$ in Eq. (4), as long as the quasiparticle excitation gap remains open at all momenta (see Supplementary Fig. 3).

TNSs are realized when 1D lines $\mathbf{Q}\cdot\mathbf{r} = n\pi/2$ become topologically inequivalent. For $\theta = 0, \pi/2$, the order parameter phase is constant $\phi = 0, \pi/2$: for $\theta = \phi = 0$, the gap closes at finite momenta in the regime where $\nu = 1$, preventing the realization of a nontrivial gapped phase; for $\theta = \phi = \pi/2$ instead, the gap is always open for $b_z \neq 0$, and TNSs may emerge when nontrivial phases are realized on the antinodal lines $\Delta(\mathbf{r}) = \Delta_0$ for $b + |m| > \sqrt{\Delta_0^2 + \mu^2} > |b - |m||$, and trivial phases on the nodal lines $\Delta(\mathbf{r}) = 0$ for $|b - |m|| > |\mu|$ (nodal lines are $\Delta(\mathbf{r}) = 0$ and thus cannot realize a nontrivial TS). However, this phase is not physical since the superconductivity can only be realized when the Fermi level lies within the conduction band, i.e., for $|\mu| > b - |m|$. For $\theta \approx \pi/4$ instead, the order parameter is $\Delta(\mathbf{r}) \approx \Delta_0/\sqrt{2}$ which corresponds to trivial and nontrivial phases with $\phi(\mathbf{r}) = \mathbf{Q}\cdot\mathbf{r} = 0, \pi/2 \bmod \pi$, respectively, provided that

$$2|m|\sqrt{\mu^2 + \Delta_0^2/2} > |m^2 + \mu^2 + \Delta_0^2/2 - b^2| > 2|m||\mu|, \tag{6}$$

as it follows from Eq. (4). The resulting TNSs are quasi-1D nontrivial regions close to the 1D lines $\mathbf{Q}\cdot\mathbf{r} = \pi n$ parallel to the in-plane field and effectively equivalent to 1D TSs. If stripes extend along the whole surface, reaching the hinges, there will be a MM at each end of the stripe, as in Fig. 1c. These end modes can also be seen as the corner modes of the effectively 2D TSs obtained by extending the 1D lines along the z direction, resulting in 2D planes parallel to the in-plane field and the z-axis, cutting the 3D TI into 2D slices. Hence, the confinement of the 2D boundary Hamiltonian into a 1D Hamiltonian describing the TNSs corresponds to the confinement of the surface states of a 3D second-order topological phase (with hinge modes) into the edge states of a 2D second-order topological phase with corner modes defined by the planes with $\mathbf{Q}\cdot\mathbf{r} = \pi n$.

The formation of quasi-1D topological superconducting stripes and pointlike MMs at their ends is a consequence of dimensional reduction[70]. The quasi-1D stipes are indeed narrow 2D regions which are topologically nontrivial, with a length determined by the system size (or by the presence of domain walls) and a width $d < \lambda/2$ coinciding with the width of the region where the phase of the order parameter ϕ is such that $\nu = 1$ in Eq. (4). If their width is comparable with their length, these 2D nontrivial regions will exhibit 1D edge modes at their border on all four sides; however, when their width becomes narrow enough, the edge states along two opposite sides will come closer and begin to overlap in space, opening a finite energy gap as a result of their finite overlap. In particular, if the width is smaller or comparable to the Majorana localization length $d \lesssim \xi$, only a single quantization channel will become available. In this regime, only a single pointlike mode may exist at each end of the stripe. The dimensional reduction from a 2D to a 1D topological state requires stripes with a width smaller than their length and smaller than the Majorana localization length so that only one single 1D channel is present. On the other hand, their spatial separation, given by the distance between neighboring stripes, must be larger than or comparable to the Majorana localization length $\lambda/2 \gtrsim \xi$ so that MMs remain spatially separated. Generally, one has $\xi \sim b/\Delta$ for 1D TSs[71,72].

As explained, symmetry arguments alone restrict the possible states to $\theta = 0, \pi/2$ (LO states) and $\theta = \pi/4$ (FF state), but only the FF state with $\theta = \pi/4$ can exhibit TNSs. We find numerical evidence that the state that fulfills the self-consistence equation at zero temperature has an order parameter which is approximately equal to Eq. (5) with $\theta = \pi/4$. Indeed, we calculate the order parameter self-consistently at zero temperature and as a function of the spatial coordinate as $\Delta_\tau(\mathbf{r}) = -U\langle 0|\psi_{\tau\downarrow}(\mathbf{r})\psi_{\tau\uparrow}(\mathbf{r})|0\rangle$ using Eq. (5) with several choices of θ and with $Q = 2b_{xy}/v$ as the initial guess of the self-consistent calculation for realistic choices of the system parameters for Bi_2Te_3[73], proximitized with NbTiN or $NbSe_2$, compatible with Eq. (6). The resulting order parameter obtained self-consistently at zero temperature is approximately equal to Eq. (5) with $\theta = \pi/4$, corresponding to an FF order with almost constant magnitude and nonuniform phase, excluding regions close to the boundaries of the system, where the magnitude of the order parameter is slightly suppressed. This result is in agreement with the results of ref. 58, which found that FFLO states with $\theta \approx \pi/4$ are stable also at finite temperature and for large in-plane magnetic fields b_{xy} (The ansatz for the order parameter in Eq. (5), which describes a generic FFLO state interpolating between an FF state (for $\theta = 0, \pi/2$) and an LO state (for $\theta = \pi/4$) coincides with the ansatz in ref. 58, where the order parameter is parameterized in terms of $b = \cos(\theta)$. In ref. 58, it is found $b = 0.77$, which is approximately equal to $b = \cos(\theta) = \cos(\pi/4) = 1/\sqrt{2} \approx 0.707$, indicating an LO state although, in that paper, the state is always called an FF state for any choice of b). Therefore, the superconducting order self-tunes to support the TNS phase, which is therefore a self-organized topological state, in this regard analogous to magnetic adatom chains with a spin helical order self-tuned to support the topological phase[74]. Figure 2a shows the local density of states (LDOS) at zero energy in the TNSs regime calculated numerically. The peaks in the LDOS indicate MMs localized at the ends of the 1D TNSs at $\phi(\mathbf{r}) = \pm\pi/2$.

Manipulation of topologically nontrivial stripes

TNSs can be manipulated in several ways. Rotating the magnetic field around the z-axis (perpendicular to the surface) changes the in-plane field direction and hence the stripes direction, while rotating the field in the xy-

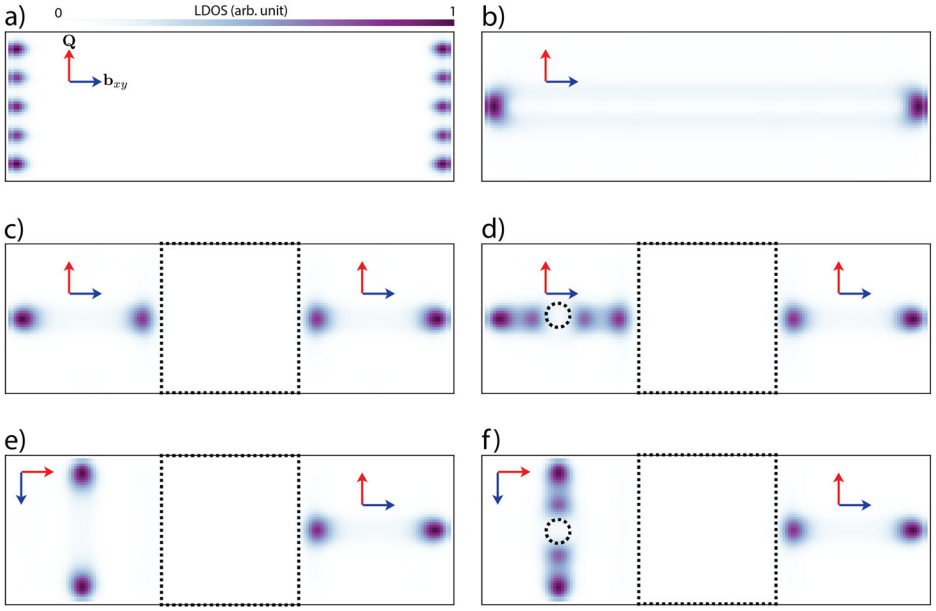

Fig. 2 | Local density of states (LDOS) at zero energy calculated numerically for a proximitized topological insulator film in the inhomogeneous superconducting phase in a system of size 162 × 54 lattice sites with open boundary conditions. **a** Topologically nontrivial stripes corresponding to the order parameter phase $\phi(\mathbf{r}) = \pm\,\pi/2$ with Majorana modes at their ends separated by a distance $\lambda/2 = \pi/Q \approx \pi v/2b_{xy}$. **b** A single stripe obtained by tuning the in-plane field such that λ is approximately equal to the width of the system. **c** same as (**b**), but with a trivial region in the middle, acting as a domain wall splitting the stripe into two. **d** same as (**c**), but with an additional trivial region on the left, acting as a pointlike defect further splitting the left stripe into two. **e** and **f** same as (**c**) and (**d**), but rotating the in-plane field on the left, (**e**) rotating the stripe, and (**f**) rotating two stripes around each other. Arrows indicate the direction of the Cooper pair momentum **Q** and of the in-plane field $\mathbf{b}_{xy}$. Areas enclosed by dotted lines indicate regions with $\mu = 0$ suppressing the superconducting order. The order parameter, calculated self-consistently, is compatible with $\theta = \pi/4$ in Eq. (5).

plane changes the in-plane field magnitude and hence the distance $\lambda/2$ between the stripes. Moreover, topologically trivial regions $v = 0$ can behave as domain walls or pointlike defects that confine the stripes or split a single stripe into two. Trivial regions can be created by locally increasing the tunneling m between the two TI surfaces (by locally modifying the TI layer thickness), such that $|m| \gg |\mu|$, $|\Delta|$, $|b|$ or, alternatively, decreasing the chemical potential $|\mu| < b - |m|$ by using external gates, driving the Fermi level out of the conduction band and thus suppressing the superconducting order, so that the first term in Eq. (4) dominates. Trivial regions can also be created by suppressing the magnetic field since Eq. (4) yields $v = 0$ for $b = 0$. Furthermore, isolated stripes are obtained by tuning the distance $\lambda/2$ such that only a single stripe fits within the TNS phase (confined by the system edges or by domain walls), as in Fig. 2b.

Multilocational modes, SUSY, SYK model, and Yang-Lee anyons

MMs at the ends of TNSs hybridize within a low-energy manifold of dimension $2N$, forming highly nonlocal modes delocalized over spatially separated points described by the effective Hamiltonian

$$\mathcal{H}_{\rm eff} = \mathrm{i}w\sum_{n=1}^{N-1}\sum_{s=L,R}\gamma_{s,n}\gamma_{s,n+1} + \mathrm{i}w'\sum_{n=1}^{N}\gamma_{L,n}\gamma_{R,n}, \tag{7}$$

with $\gamma_{L,n}$ and $\gamma_{R,n}$ the modes on the left and right ends, $w \propto \mathrm{e}^{-\lambda/2\xi}$ and $w\prime \propto \mathrm{e}^{-l/\xi}$ the couplings between modes on the same side (at a distance $\lambda/2$) and on opposite sides of the stripes (at a distance l), respectively, with $w, w'>0$ up to a gauge transformation. This manifold can exhibit nonlocal fermionic modes at exactly zero energy, even at finite sizes. For $N \to \infty$ (or equivalently, in a setup with periodic boundaries), the MMs realize two translationally invariant lattices which are decoupled for $w\prime = 0$. In this case, the N MMs of each lattice are degenerate under translations and hybridize into two MMs $\widetilde{\gamma}_{1,2}$ (forming a single fermionic mode) at zero energy, delocalized into N spatially separated points corresponding to the ends of the TNSs. This results in quantum mechanical SUSY[14] or space-time SUSY in the presence of many-body interactions[12,13,16]. For $w'>0$, the two fermionic modes (one for each side) hybridize at finite energy. The fractionalization of the fermionic degrees of freedom and the emergence of quantum-mechanical SUSY is also observed in finite systems $N < \infty$ with open boundary conditions. Indeed, we find that if $w = w'$ and $N = 3m + 2 = 2, 5, 8, \ldots$, the two nonlocal modes

$$\widetilde{\gamma}_1 = \frac{1}{\sqrt{2m+2}}\sum_{n=0}^{m}\kappa_n(\gamma_{L,3n+1} + \gamma_{R,3n+2}) + \kappa_{n-1}(\gamma_{R,3n+1} - \gamma_{L,3n+2}), \tag{8}$$

$$\widetilde{\gamma}_2 = \frac{1}{\sqrt{2m+2}}\sum_{n=0}^{m}\kappa_n(\gamma_{R,3n+1} - \gamma_{L,3n+2}) + \kappa_{n+1}(\gamma_{L,3n+1} + \gamma_{R,3n+2}), \tag{9}$$

with $\kappa_n = \cos(n\pi/2)$, have exactly zero energy, each delocalized into $2(m + 1) = 2(N + 1)/3$ spatially separated points. This regime $w' = w$ is realized when the length of the stripes is comparable with the distance between mutual stripes (see Supplementary Note 6). This setup can be advantageous when the system dimensions cannot be stretched indefinitely. Also, we find that if $w' \to 0$ and $N = 2m + 1$, the two nonlocal modes

$$\begin{aligned}\widetilde{\gamma}_1 &= \tfrac{1}{\sqrt{m+1}}\sum_{n=0}^{m}\gamma_{L,2n+1},\\ \widetilde{\gamma}_2 &= \tfrac{1}{\sqrt{m+1}}\sum_{n=0}^{m}\gamma_{R,2n+1},\end{aligned} \tag{10}$$

have exactly zero energy, each delocalized into $m + 1 = (N + 1)/2$ spatially separated points at the ends of every other stripe. This case is realized in Fig. 2a since $w'\approx 0$ (see Supplementary Fig. 4). The case $w\prime = 0$ is realized asymptotically when the stripes become infinitely long. Hence, this case requires one of the system dimensions to be much larger than the other. These two cases are further examples of multi-locational MMs recently predicted to appear in three-terminal Josephson junctions[60]. In all these cases, the groundstate is twofold degenerate, with two nonlocal MMs $\widetilde{\gamma}_1$ and $\widetilde{\gamma}_2$ forming a single zero-energy and particle-hole symmetric fermionic mode. One can thus define two fermionic operators $Q_{1,2} = \widetilde{\gamma}_{1,2}\sqrt{H_{\rm SUSY}}$ satisfying the algebra $\{P, Q_i\} = 0$, $\{Q_i, Q_j\} = 2\delta_{ij}H_{\rm SUSY}$, where $H_{\rm SUSY}$ is the many-body Hamiltonian with all energy levels positive (obtained by adding a positive constant) and P the fermion parity operator. This corresponds to spontaneously broken $\mathcal{N} = 2$ quantum mechanical SUSY[75] with supercharges $Q_{1,2}$, zero superpotential, and Witten index $W = 1$. Furthermore, configurations with several stripes, as in Fig. 2(a), are equivalent to sets of equally-spaced 1D TSs, which can effectively realize the SYK model when

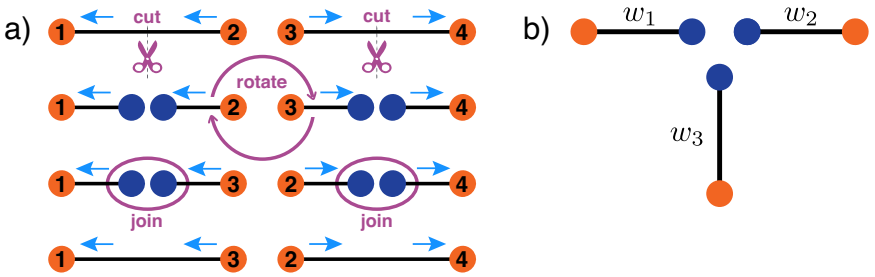

Fig. 3 | Possible braiding protocols. a Rotating left and right stripes exchange the modes γ_1, γ_2 and γ_3, γ_4, respectively. Exchanging γ_2, γ_3 is obtained following a three steps protocol (from top to bottom): i) cut two stripes with antiparallel fields into four (creating four additional Majorana modes), ii) rotate the resulting two inner stripes one around the other, following the arrows, leaving the other two outer stripes unchanged, and iii) join the two inner stripes to the outer stripes. Arrows indicate the direction of the in-plane field. **b** Braiding can also be performed in parameter space arranging three topologically nontrivial stripes around a pointlike defect and controlling the couplings $w_{1,2,3}$ between Majorana modes on opposite ends of the stripes, without moving them.

coupled to a quantum dot[22], or Yang-Lee anyons when coupled to a metallic bath[61], provided that the single-particle couplings w and w' are suppressed[76]. Finally, note that for $N \to \infty$, the two MMs chains at opposite edges form a pair of 1D chiral Majorana edge modes with finite dispersion[17,58,62].

Braiding

MMs at the ends of TNSs can be braided. To do so, we need the ability to i) rotate stripes to exchange the MMs and ii) split or merge stripes to implement fusion and read-out. TNSs can be rotated by rotating the in-plane field. Adiabatically decreasing the chemical potential (thus suppressing superconductivity) on specified regions can create domain walls or pointlike defects that split single stripes into two stripes with parallel magnetic fields. The reverse process merges two stripes with parallel fields into one. Figures 2c, d show how to adiabatically split a single stripe into two segments via a domain wall in the middle, and rotate one segment by rotating the in-plane field in one half of the system. Figures 2e, f show how to rotate two stripes around a central pointlike defect. The lowest energy levels corresponding to the MMs remained close to zero in all cases (see Supplementary Figs. 6 and 7). Figure 3a illustrates a possible braiding protocol. Additionally, TNSs can be controlled by moving the domain walls. Alternatively, braiding can be performed in parameter space[77,78] without moving the TNSs, e.g., arranging three TNSs around a pointlike defect as in Fig. 3b and controlling the coupling between MMs on opposite ends of the TNSs (see Supplementary Fig. 8).

Discussion

In this work, we described an alternative 2D platform to create, manipulate, and braid MMs via inhomogeneous superconducting orders in proximitized TIs. Unlike other 2D platforms, MMs do not localize at the vortex cores of the order parameter but at the opposite ends of TNSs induced by the inhomogeneous order. This setup can realize topological quantum gates and other exotic quantum phenomena, such as quantum mechanical SUSY, Yang-Lee anyons, and the SYK model. Moreover, TNSs may also be induced by inhomogeneous superconducting orders in Sr_2RuO_4[79], iron pnictides[80], organic superconductors[81–83], $SrTiO_3/LaAlO_3$ interfaces[84], $KTaO_3$/EuO or $KTaO_3/LaAlO_3$ interfaces in the inhomogeneous superconducting stripe phase[85], and two-component cold atomic Fermi gases with population imbalance and effective spin-orbit coupling[62,86–90]. Finally, the experimental detection of TNSs would also provide indirect evidence of FFLO inhomogeneous superconductivity.

Methods

The numerical results were obtained by discretizing the continuous Hamiltonian into a lattice model and calculating the energy spectra, wavefunction, and superconducting order parameter self-consistently at zero temperature. The LDOS at zero energy was calculated directly from the energy spectra and wavefunction. The parameters used for the numerical calculations were chosen to be compatible with heterostructures of Bi_2Te_3[73] proximitized with NbTiN or $NbSe_2$. The topological invariants (Chern numbers) were calculated numerically using the Fukui-Hatsugai-Suzuki method[67], while the parity of the topological invariants was calculated as the sign of the product of the Pfaffians of the Hamiltonian in the Majorana basis with momenta spanning the time-reversal symmetry points in the Brillouin zone.

Data availability

The code used for the numerical simulations within this paper and the resulting data are available from the corresponding author upon reasonable request.

Received: 5 February 2024; Accepted: 29 July 2024;
Published online: 10 August 2024

References

1. Read, N. & Green, D. Paired states of fermions in two dimensions with breaking of parity and time-reversal symmetries and the fractional quantum Hall effect. *Phys. Rev. B* **61**, 10267 (2000).
2. Kitaev, A. Y. Unpaired Majorana fermions in quantum wires. *Phys. Usp.* **44**, 131 (2001).
3. Fu, L. & Kane, C. Superconducting proximity effect and Majorana fermions at the surface of a topological insulator. *Phys. Rev. Lett.* **100**, 096407 (2008).
4. Sato, M., Takahashi, Y. & Fujimoto, S. Non-abelian topological order in *s*-wave superfluids of ultracold fermionic atoms. *Phys. Rev. Lett.* **103**, 020401 (2009).
5. Sato, M. & Fujimoto, S. Topological phases of noncentrosymmetric superconductors: edge states, Majorana fermions, and non-Abelian statistics. *Phys. Rev. B* **79**, 094504 (2009).
6. Lutchyn, R., Sau, J. & Das Sarma, S. Majorana fermions and a topological phase transition in semiconductor-superconductor heterostructures. *Phys. Rev. Lett.* **105**, 077001 (2010).
7. Oreg, Y., Refael, G. & Von Oppen, F. Helical liquids and Majorana bound states in quantum wires. *Phys. Rev. Lett.* **105**, 177002 (2010).
8. Ivanov, D. A. Non-abelian statistics of half-quantum vortices in *p*-wave superconductors. *Phys. Rev. Lett.* **86**, 268 (2001).
9. Kitaev, A. Fault-tolerant quantum computation by anyons. *Ann. Phys.* **303**, 2 (2003).
10. Stern, A., Von Oppen, F. & Mariani, E. Geometric phases and quantum entanglement as building blocks for non-abelian quasiparticle statistics. *Phys. Rev. B* **70**, 205338 (2004).
11. Nayak, C., Simon, S., Stern, A., Freedman, M. & Das Sarma, S. Non-abelian anyons and topological quantum computation. *Rev. Mod. Phys.* **80**, 1083 (2008).
12. Rahmani, A., Zhu, X., Franz, M. & Affleck, I. Phase diagram of the interacting Majorana chain model. *Phys. Rev. B* **92**, 235123 (2015).

13. Rahmani, A., Zhu, X., Franz, M. & Affleck, I. Emergent supersymmetry from strongly interacting Majorana zero modes. *Phys. Rev. Lett.* **115**, 166401 (2015).
14. Hsieh, T. H., Halász, G. B. & Grover, T. All Majorana models with translation symmetry are supersymmetric. *Phys. Rev. Lett.* **117**, 166802 (2016).
15. Huang, Z., Shimasaki, S. & Nitta, M. Supersymmetry in closed chains of coupled Majorana modes. *Phys. Rev. B* **96**, 220504(R) (2017).
16. Sannomiya, N. & Katsura, H. Supersymmetry breaking and Nambu-Goldstone fermions in interacting Majorana chains. *Phys. Rev. D* **99**, 045002 (2019).
17. Marra, P., Inotani, D. & Nitta, M. 1D Majorana Goldstinos and partial supersymmetry breaking in quantum wires. *Commun. Phys.* **5**, 149 (2022).
18. Marra, P., Inotani, D. & Nitta, M. Dispersive one-dimensional Majorana modes with emergent supersymmetry in one-dimensional proximitized superconductors via spatially modulated potentials and magnetic fields. *Phys. Rev. B* **105**, 214525 (2022).
19. Miura, U., Shimomura, K. & Totsuka, K. Interacting Kitaev chain with $\mathcal{N}=1$ supersymmetry. *Phys. Rev. B* **109**, 085141 (2024).
20. Sachdev, S. & Ye, J. Gapless spin-fluid ground state in a random quantum Heisenberg magnet. *Phys. Rev. Lett.* **70**, 3339 (1993).
21. Kitaev, A. Talks at KITP, on April 7 and May 27 (unpublished).
22. Chew, A., Essin, A. & Alicea, J. Approximating the Sachdev-Ye-Kitaev model with Majorana wires. *Phys. Rev. B* **96**, 121119(R) (2017).
23. Alicea, J. New directions in the pursuit of Majorana fermions in solid state systems. *Rep. Prog. Phys.* **75**, 076501 (2012).
24. Leijnse, M. & Flensberg, K. Introduction to topological superconductivity and Majorana fermions. *Semicond. Sci. Technol.* **27**, 124003 (2012).
25. Tanaka, Y., Sato, M. & Nagaosa, N. Symmetry and topology in superconductors—odd-frequency pairing and edge states. *J. Phys. Soc. Jpn.* **81**, 011013 (2012).
26. Stanescu, T. & Tewari, S. Majorana fermions in semiconductor nanowires: fundamentals, modeling, and experiment. *J. Phys. Cond. Matter* **25**, 233201 (2013).
27. Beenakker, C. Search for Majorana fermions in superconductors. *Annu. Rev. Condens. Matter Phys.* **4**, 113 (2013).
28. Elliott, S. & Franz, M. Colloquium: Majorana fermions in nuclear, particle, and solid-state physics. *Rev. Mod. Phys.* **87**, 137 (2015).
29. Das Sarma, S., Freedman, M. & Nayak, C. Majorana zero modes and topological quantum computation. *npj Quantum Inf.* **1**, 15001 (2015).
30. Sato, M. & Fujimoto, S. Majorana fermions and topology in superconductors. *J. Phys. Soc. Jpn.* **85**, 072001 (2016).
31. Sato, M. & Ando, Y. Topological superconductors: a review. *Rep. Prog. Phys.* **80**, 076501 (2017).
32. Aguado, R. Majorana quasiparticles in condensed matter. *Riv. Nuovo Cim.* **40**, 523 (2017).
33. Laubscher, K. & Klinovaja, J. Majorana bound states in semiconducting nanostructures. *J. Appl. Phys.* **130**, 081101 (2021).
34. Marra, P. Majorana nanowires for topological quantum computation. *J. Appl. Phys.* **132**, 231101 (2022).
35. Masaki, Y., Mizushima, T. & Nitta, M. Non-Abelian anyons and non-Abelian vortices in topological superconductors. In *Encyclopedia of Condensed Matter Physics* 2nd edn (ed. Chakraborty, T.), pp. 755–794 (Academic Press, 2024).
36. Tanaka, Y., Tamura, S. & Cayao, J. Theory of Majorana zero modes in unconventional superconductors, *Prog. Theor. Exp. Phys*., ptae065 (2024).
37. Yuan, N. F. Q., Mak, K. F. & Law, K. T. Possible topological superconducting phases of MoS_2. *Phys. Rev. Lett.* **113**, 097001 (2014).
38. Hsu, Y.-T., Vaezi, A., Fischer, M. H. & Kim, E.-A. Topological superconductivity in monolayer transition metal dichalcogenides. *Nat. Commun.* **8**, 14985 (2017).
39. Yin, J.-X. et al. Observation of a robust zero-energy bound state in iron-based superconductor Fe(Te,Se). *Nat. Phys.* **11**, 543 (2015).
40. Zhang, P. et al. Observation of topological superconductivity on the surface of an iron-based superconductor. *Science* **360**, 182 (2018).
41. Wang, D. et al. Evidence for Majorana bound states in an iron-based superconductor. *Science* **362**, 333 (2018).
42. Huang, Z. et al. Dual topological states in the layered titanium-based oxypnictide superconductor BaTi2Sb2O. *npj Quantum Materials* **7**, 70 (2022).
43. Mascot, E., Bedow, J., Graham, M., Rachel, S. & Morr, D. K. Topological superconductivity in skyrmion lattices. *npj Quantum Materials* **6**, 6 (2021).
44. Crawford, D. et al. Majorana modes with side features in magnet-superconductor hybrid systems. *npj Quantum Materials* **7**, 117 (2022).
45. Escribano, S. D. et al. Semiconductor-ferromagnet-superconductor planar heterostructures for 1D topological superconductivity. *npj Quantum Materials* **7**, 81 (2022).
46. Wong, K. H. et al. Higher order topological superconductivity in magnet-superconductor hybrid systems. *npj Quantum Materials* **8**, 31 (2023).
47. Sau, J., Tewari, S., Lutchyn, R., Stanescu, T. & Das Sarma, S. Non-abelian quantum order in spin-orbit-coupled semiconductors: search for topological Majorana particles in solid-state systems. *Phys. Rev. B* **82**, 214509 (2010).
48. Akhmerov, A., Dahlhaus, J., Hassler, F., Wimmer, M. & Beenakker, C. Quantized conductance at the Majorana phase transition in a disordered superconducting wire. *Phys. Rev. Lett.* **106**, 057001 (2011).
49. Stanescu, T., Lutchyn, R. & Das Sarma, S. Majorana fermions in semiconductor nanowires. *Phys. Rev. B* **84**, 144522 (2011).
50. Alicea, J., Oreg, Y., Refael, G., Von Oppen, F. & Fisher, M. Non-abelian statistics and topological quantum information processing in 1D wire networks. *Nat. Phys.* **7**, 412 (2011).
51. Clarke, D., Sau, J. & Tewari, S. Majorana fermion exchange in quasi-one-dimensional networks. *Phys. Rev. B* **84**, 035120 (2011).
52. Halperin, B., Oreg, Y., Stern, A., Refael, G., Alicea, J. & Von Oppen, F. Adiabatic manipulations of Majorana fermions in a three-dimensional network of quantum wires. *Phys. Rev. B* **85**, 144501 (2012).
53. Fulde, P. & Ferrell, R. A. Superconductivity in a strong spin-exchange field. *Phys. Rev.* **135**, A550 (1964).
54. Larkin, A. I. & Ovchinnikov, Y. N. Nonuniform state of superconductors. *Zh. Eksp. Teor. Fiz*. **47**, 1136.
55. Casalbuoni, R. & Nardulli, G. Inhomogeneous superconductivity in condensed matter and QCD. *Rev. Mod. Phys.* **76**, 263 (2004).
56. Lu, H.-Z., Shan, W.-Y., Yao, W., Niu, Q. & Shen, S.-Q. Massive Dirac fermions and spin physics in an ultrathin film of topological insulator. *Phys. Rev. B* **81**, 115407 (2010).
57. Yu, R. et al. Quantized anomalous Hall effect in magnetic topological insulators. *Science* **329**, 61 (2010).
58. Hu, L.-H., Liu, C.-X. & Zhang, F.-C. Topological Larkin-Ovchinnikov phase and Majorana zero mode chain in bilayer superconducting topological insulator films. *Commun. Phys.* **2**, 25 (2019).
59. Schindler, F. et al. Higher-order topological insulators. *Sci. Adv.* **4**, eaat0346 (2018).
60. Nagae, Y., Schnyder, A. P., Tanaka, Y., Asano, Y. & Ikegaya, S., Multilocational Majorana zero modes, *Phys. Rev. B* **110**, L041110 (2024)
61. Sanno, T., Yamada, M. G., Mizushima, T. & Fujimoto, S. Engineering Yang-Lee anyons via Majorana bound states. *Phys. Rev. B* **106**, 174517 (2022).

62. Zhang, W. & Yi, W. Topological Fulde-Ferrell-Larkin-Ovchinnikov states in spin-orbit-coupled Fermi gases. *Nat. Commun.* **4**, 2711 (2013).
63. Liu, C.-X. et al. Oscillatory crossover from two-dimensional to three-dimensional topological insulators. *Phys. Rev. B* **81**, 041307(R) (2010).
64. Black-Schaffer, A. M. & Doniach, S. Self-consistent solution for proximity effect and Josephson current in ballistic graphene SNS Josephson junctions. *Phys. Rev. B* **78**, 024504 (2008).
65. Lababidi, M. & Zhao, E. Microscopic simulation of superconductor/topological insulator proximity structures. *Phys. Rev. B* **83**, 184511 (2011).
66. Bernevig, B., Hughes, T. & Zhang, S.-C. Quantum spin Hall effect and topological phase transition in HgTe quantum wells. *Science* **314**, 1757 (2006).
67. Fukui, T., Hatsugai, Y. & Suzuki, H. Chern numbers in discretized Brillouin zone: efficient method of computing (spin) Hall conductances. *J. Phys. Soc. Jpn.* **74**, 1674 (2005).
68. Tewari, S. & Sau, J. Topological invariants for spin-orbit coupled superconductor nanowires. *Phys. Rev. Lett.* **109**, 150408 (2012).
69. Budich, J. C. & Ardonne, E. Equivalent topological invariants for one-dimensional Majorana wires in symmetry class D. *Phys. Rev. B* **88**, 075419 (2013).
70. Potter, A. & Lee, P. Multichannel generalization of Kitaev's Majorana end states and a practical route to realize them in thin films. *Phys. Rev. Lett.* **105**, 227003 (2010).
71. Klinovaja, J. & Loss, D. Composite Majorana fermion wave functions in nanowires. *Phys. Rev. B* **86**, 085408 (2012).
72. Mishmash, R., Aasen, D., Higginbotham, A. & Alicea, J. Approaching a topological phase transition in Majorana nanowires. *Phys. Rev. B* **93**, 245404 (2016).
73. Chen, Y. L. et al. Experimental realization of a three-dimensional topological insulator Bi_2Te_3. *Science* **325**, 178 (2009).
74. Vazifeh, M. & Franz, M. Self-organized topological state with Majorana fermions. *Phys. Rev. Lett.* **111**, 206802 (2013).
75. Witten, E. Dynamical breaking of supersymmetry. *Nucl. Phys. B.* **188**, 513 (1981).
76. García-García, A. M., Loureiro, B., Romero-Bermúdez, A. & Tezuka, M. Chaotic-integrable transition in the Sachdev-Ye-Kitaev model. *Phys. Rev. Lett.* **120**, 241603 (2018).
77. Sau, J., Clarke, D. & Tewari, S. Controlling non-abelian statistics of Majorana fermions in semiconductor nanowires. *Phys. Rev. B* **84**, 094505 (2011).
78. Karzig, T., Pientka, F., Refael, G. & Von Oppen, F. Shortcuts to non-abelian braiding. *Phys. Rev. B* **91**, 201102(R) (2015).
79. Kinjo, K. et al. Superconducting spin smecticity evidencing the Fulde-Ferrell-Larkin-Ovchinnikov state in Sr_2RuO_4. *Science* **376**, 397 (2022).
80. Kasahara, S. et al. Evidence for an Fulde-Ferrell-Larkin-Ovchinnikov state with segmented vortices in the BCS-BEC-crossover superconductor FeSe. *Phys. Rev. Lett.* **124**, 107001 (2020).
81. Coniglio, W. A. et al. Superconducting phase diagram and FFLO signature in λ-$(BETS)_2GaCl_4$ from rf penetration depth measurements. *Phys. Rev. B* **83**, 224507 (2011).
82. Sugiura, S. et al. Fulde–Ferrell–Larkin–Ovchinnikov and vortex phases in a layered organic superconductor. *npj Quantum Mater.* **4**, 7 (2019).
83. Sari, D. P. et al. Distorted superconducting nodal line on a single Fermi surface in the anisotropic organic superconductor $\lambda - (BETS)_2GaCl_4$. *Phys. Rev. B* **104**, 224506 (2021).
84. Michaeli, K., Potter, A. C. & Lee, P. A. Superconducting and ferromagnetic phases in $SrTiO_3/LaAlO_3$ oxide interface structures: possibility of finite momentum pairing. *Phys. Rev. Lett.* **108**, 117003 (2012).
85. Liu, C. et al. Two-dimensional superconductivity and anisotropic transport at $KTaO_3$ (111) interfaces. *Science* **371**, 716 (2021).
86. Zwierlein, M. W., Schirotzek, A., Schunck, C. H. & Ketterle, W. Fermionic superfluidity with imbalanced spin populations. *Science* **311**, 492 (2006).
87. Takahashi, M., Mizushima, T., Ichioka, M. & Machida, K. Vortex-core structure in neutral fermion superfluids with population imbalance. *Phys. Rev. Lett.* **97**, 180407 (2006).
88. Suzuki, K. M., Mizushima, T., Ichioka, M. & Machida, K. Magnetization profile and core-level spectroscopy in a multiply quantized vortex of imbalanced Fermi superfluids. *Phys. Rev. A* **77**, 063617 (2008).
89. Qu, C. et al. Topological superfluids with finite-momentum pairing and Majorana fermions. *Nat. Commun.* **4**, 2710 (2013).
90. Inotani, D., Yasui, S., Mizushima, T. & Nitta, M. Radial Fulde-Ferrell-Larkin-Ovchinnikov-like state in a population-imbalanced Fermi gas. *Phys. Rev. A* **103**, 053308 (2021).

Acknowledgements

P.M. thanks Paolo Mele, Dita Puspita Sari, Masatoshi Sato, and Ken Shiozaki for useful discussions, and Maria Bartho for help preparing figures. P.M. is supported by the Japan Science and Technology Agency (JST) of the Ministry of Education, Culture, Sports, Science and Technology (MEXT), JST CREST Grant no. JPMJCR19T2, the Japan Society for the Promotion of Science (JSPS) Grant-in-Aid for Early-Career Scientists KAKENHI Grant No. JP23K13028 and No. JP20K14375. T.M. is supported by the Grant-in-Aid for Scientific Research on Innovative Areas "Quantum Liquid Crystals" Grant no. JP22H04480 and JSPS KAKENHI Grant No. JP20K03860, no. JP21H01039, and No. JP22H01221. M.N. is supported by JSPS KAKENHI Grant no. JP22H01221 and by the WPI program "Sustainability with Knotted Chiral Meta Matter (SKCM2)" at Hiroshima University.

Author contributions

All authors P.M., D.I., T.M., and M.N. contributed to the scientific discussion and to the final revision of the manuscript. P.M. carried out the numerical calculations and wrote the initial draft.

Competing interests

The authors declare no competing interests.

Additional information

Supplementary information The online version contains supplementary material available at https://doi.org/10.1038/s41535-024-00672-0.

Correspondence and requests for materials should be addressed to Pasquale Marra.